ELSEVIER

Dyes and Pigments 52 (2002) 101–114

DYES and PIGMENTS

www.elsevier.com/locate/dyepig

The synthesis and properties of some carboxy-substituted analogs of butter yellow

William E. Brenzovich, Jr., Ronald J. T. Houk, Sienna M. A. Malubay, Joshua O. Miranda, Katherine M. Ross, Christopher J. Abelt*

Department of Chemistry, College of William and Mary, Williamsburg, VA 23187-8795, USA

Received 20 February 2001; received in revised form 12 June 2001; accepted 2 November 2001

Abstract

A seven step synthesis of 3,3′-bis(carbomethoxy)-4,4′-bis-(dimethylamino)-azobenzene from anthranilic acid is described. It has been found that the carbomethoxy groups affect the required oxidative azo coupling and methylation steps. Perborate coupling of 2-carbomethoxy-*N*-acetyl-*p*-phenylenediamine gives the corresponding azo compound in good yield, but the reaction also produces variable amounts of an azoxy compound. Tetramethylation of 3,3′-bis(carbomethoxy)-4,4′-diaminoazobenzene requires forcing conditions [$(CH_3O)_2SO_2$ at 160 °C]. Protonation of 3,3′-bis(carbomethoxy)-4,4′-bis-(dimethylamino)azobenzene gives the ammonium ion tautomer because the carbomethoxy groups force the adjacent dimethylamino groups out-of-plane. In contrast, protonation of 3,3′-bis(carbomethoxy)-4,4′-diaminoazobenzene and 4,4′-bis(dimethylamino)azobenzene-3,3′-dicarboxylic acid gives the azonium ion tautomer.

Keywords: Azo dyes; Synthesis; Aryl amine oxidation; Perborate; Azonium–ammonium tautomerization

1. Introduction

In connection with a project involving capping of β-cyclodextrin with an indicator molecule, we sought an azo dye that has C_2 symmetry, a relatively high pK_a and carboxy groups, to make two covalent linkages with the cyclodextrin. Ultimately, we chose 3,3′-bis(carbomethoxy)-4,4′-bis (dimethylamino)azobenzene (**1**), an analog of butter yellow (*N,N*-dimethyl-*p*-phenylazoaniline) as our target. The present paper pertains to the synthesis and properties of compound **1** and several structurally related intermediates. Special attention is given to some of the synthetic hurdles we encountered, most of which were caused by the presence of carbomethoxy groups.

2. Experimental

2.1. General

^{1}H NMR spectra were obtained using a Varian Mercury VX-400 spectrometer and UV/visible spectra were recorded on a Beckman DU-70 instrument. The pK_a values for dyes **1**, **8** and **9** were determined by titration with aq. HCl at the wavelengths corresponding to the absorption

* Corresponding author. Tel.: +1-757-221-2551; fax: +1-757-221-2715.

E-mail address: cjabel@wm.edu (C.J. Abelt).

0143-7208/02/$ - see front matter
PII: S0143-7208(01)00094-8

bands and no correction for ionic strength variation was made. Melting points were taken on a Thomas–Hoover capillary melting point apparatus and are uncorrected. TLC was carried out using 0.25-mm HLF precoated silica gel plates (Analtech). Combustion analysis was performed by Desert Analytics.

AM1 and PM3 calculations were performed using PC Spartan Pro® software from Wavefunction, Inc. The default program parameters were used, except C_2 symmetry was enforced, using 0–0° and 180–180° rotomers of **1**, **8** and **9**.

2.2. Synthesis

2.2.1. N-Acetylanthranilic acid

Anthranilic acid (27.4 g, 200 mmol) is added to acetic anhydride (100 ml) and the mixture is stirred overnight. The solution is poured into ice-water mixture and the resultant white solid is collected by suction filtration. The solid is air-dried, giving 31.86 g (89%) of the acetylated product that is pure enough for use in the next step.

2.2.2. Methyl N-acetylanthranilate

N-Acetylanthranilic acid (34.43 g, 192 mmol) is combined with aqueous sodium bicarbonate (250 ml, 10%) and 95% ethanol (150 ml) and the solution is warmed to 30 °C. Dimethyl sulfate (28 ml, 296 mmol) is added rapidly after CO_2 evolution has subsided. The reaction mixture is heated to 45 °C over 1 h, stirred overnight at room temperature, and poured into a rapidly stirring mixture of ice and brine. The solid is collected by suction filtration and air-dried. The dry solid (31.8 g, 99%) is pure enough for use in the next step.

2.2.3. 2-Carbomethoxy-4-nitroacetanilide

Nitric acid (140 ml) is added slowly and with stirring to conc. sulfuric acid (140 ml) with water bath cooling so that the temperature does not rise above 25 °C. The acid mixture is cooled below 0 °C in an ice-salt bath and methyl *N*-acetylanthranilate (31.9 g, 165 mol) is added portionwise, at a rate such that the temperature does not rise above 0 °C. The reaction mixture is allowed to warm to room temperature over 2 h and added dropwise into rapidly stirring ice-cooled water (700 ml). The solid that forms is collected by suction filtration on a sintered glass funnel and washed with water until the wash water was acid free. The solid is air-dried and recrystallised from a minimum volume of acetone (~300 ml) giving 14.75 g product in the first crop and 5.39 g in the second crop (51%). The product remaining in the mother liquors is mainly the 6-nitro isomer.

2.2.4. 2-Carbomethoxy-N-acetyl-p-phenylenediamine

A Parr hydrogenation bottle is charged with 2-carbomethoxy-4-nitroacetanilide (14.75 g, 61.9 mmol), 95% EtOH (300 ml, 95%), and 10% Pd/C catalyst (1 g). The bottle is pressurized with hydrogen (54 psi) and the hydrogenation is allowed to proceed overnight. The mixture of product and catalyst is collected by suction filtration and then washed with acetone (200 ml). The combined filtrates are concentrated in vacuo and the precipitate is collected by suction filtration, giving 10.98 g (85%) product after drying in vacuo, m.p. 155–157 °C. ^{1}H NMR ($CDCl_3$): 10.66 (*br s*, 1H), 8.48 (*d*, $J=8.9$ Hz, 1H), 7.33 (*d*, $J=2.8$ Hz, 1H), 6.90 (*dd*, $J=2.8$, 8.9 Hz, 1H), 3.90 (*s*, 3H), 2.20 (*s*, 3H). ^{13}C NMR ($CDCl_3$): 168.6, 168.5, 141.6, 133.7, 122.2, 121.7, 116.2, 116.1, 52.4, 25.5. UV (EtOH): $\lambda_{max}=370$ nm (log $\varepsilon=4.5$).

2.2.5. 3,3′-Bis(carbomethoxy)-4,4′-bis(acetylamino)azobenzene

2.2.5.1. Perborate method. Sodium perborate tetrahydrate (1.56 g, 10.1 mmol) is added in three equal portions at 20-min intervals to a solution of 2-carbomethoxy-*N*-acetyl-*p*-phenylenediamine (2.07 g, 10.0 mmol) and boric acid (0.52 g, 8.4 mmol) in acetic acid (14 ml), at 58 °C. The reaction mixture is held at 58 °C for 6 h, cooled and then poured into ice water (250 ml). The solid is collected by suction filtration, washed with water and air-dried. Further drying in vacuo leaves 1.31 g (64%), m.p. 297–300 °C. ^{1}H NMR ($CDCl_3$): 11.27 (*br. s*, 2H), 8.89 (*d*, $J=8.9$ Hz, 2H), 8.62 (*d*, $J=2.4$ Hz, 2H), 8.13 (*dd*, $J=2.4$, 8.9 Hz, 2H), 4.00 (*s*, 6H), 2.29 (*s*, 6H). ^{13}C NMR ($CDCl_3$): 169.3, 168.8, 147.3, 143.9, 128.4, 126.7, 121.0, 115.4, 52.8, 25.8. UV (EtOH): $\lambda_{max}=370$ nm (log $\varepsilon=4.5$).

2.2.5.2. Lead tetraacetate method. To a solution of 2-carbomethoxy-*N*-acetyl-*p*-phenylenediamine (2.08 g, 10.0 mmol) in acetic acid (25 ml) is added lead tetraacetate (9.70 g, 10.1 mmol), during which time the temperature of the reaction rises to 38 °C. The reaction is stirred overnight, sodium perborate tetrahydrate (1.0 g, 6.5 mmol) is added, and stirring is continued for another night. The solid that forms is collected by filtration, washed with a small volume of HOAc and then with water until the wash water is colorless. The solid is air-dried and then dried in vacuo leaving 0.50 g (24%).

2.2.6. 3,3′-Bis(carbomethoxy)-4,4′-diaminoazobenzene

3,3′-Bis(carbomethoxy)-4,4′-bis(acetylamino)azo benzene (3.96 g, 9.60 mmol) is suspended in MeOH (200 ml). H_2SO_4 (25 ml, 18 M) is added dropwise with external ice bath cooling and the reaction mixture is stirred at reflux overnight. The reaction mixture is allowed to cool, and is added dropwise to a rapidly stirred mixture of ice water (400 ml) and sodium bicarbonate (50 g). The solid is collected by suction filtration, air-dried and dried in vacuo to give 1.91 g (61%), m.p. 251–252 °C (dec.). ^{1}H NMR ($CDCl_3$): 8.45 (*d*, $J=2.1$ Hz, 2H), 7.89 (*dd*, $J=8.8$, 2.1 Hz, 2H), 6.73 (*d*, $J=8.8$ Hz, 2H), 6.10 (*br. s*, 4H), 3.93 (*s*, 6H). ^{13}C NMR ($CDCl_3$): 168.6, 152.2, 143.9, 129.0, 126.8, 117.2, 116.4, 51.8; UV (EtOH): $\lambda_{max}=364$ nm (log $\varepsilon=4.2$).

*2.2.7. 3,3′-Bis(carbomethoxy)-4,4′-bis(dimethylamino)azobenzene (**1**)*

3,3′-Bis(carbomethoxy)-4,4′-diaminoazobenzene (3.26 g, 9.93 mmol) is covered with dimethylsulfate (10 ml, 106 mmol) and placed under N_2. The mixture is immersed into a pre-heated oil bath (160 °C), stirred for 12 min, and allowed to cool. The resultant reaction mixture is poured into ice-cold aqueous $NaHCO_3$ and stirred overnight. The mixture is extracted twice with CH_2Cl_2 and the combined extracts are dried over $MgSO_4$ and concentrated in vacuo leaving 2.56 (67%). Column chromatography on silica gel using a gradient elution (5–50% EtOAc/hexanes) afford the azoxy compound side product from the azo coupling reaction, $R_f=0.45$ (25% EtOAc/hexanes) and the target compound (R_f 0.27) 0.82 g (21%). Recrystallisation of **1** from hexanes/CH_2Cl_2 (1:1) gave product with m.p. 140–142 °C. ^{1}H NMR ($CDCl_3$): 8.23 (*d*, $J=2.4$ Hz, 2H), 7.90 (*dd*, $J=8.9$, 2.4 Hz, 2H), 6.97 (*d*, $J=8.9$ Hz, 2H), 3.94 (*s*, 6H), 2.98 (*s*, 12H). ^{13}C NMR ($CDCl_3$): 168.8, 153.3, 144.4, 127.7, 126.1, 119.1, 116.2, 52.4, 43.5. UV (MeOH): $\lambda_{max}=425$ nm (log $\varepsilon=4.4$). Anal. calcd. for $C_{20}H_{24}N_4O_4$: C, 62.49; H, 6.29; N, 14.57. Found: C, 62.08; H, 6.11; N, 14.32.

*2.2.8. 4,4′-Bis(dimethylamino)azobenzene-3,3′-dicarboxylic acid (**9**)*

3,3′-Bis(carbomethoxy)-4,4′-bis(dimethylamino)azobenzene (0.82 g, 2.1 mmol) is added to a solution of KOH (0.37 g, 8.8 mmol) in EtOH (50 ml) and the reaction mixture is stirred at reflux for 1 h. After the solution is cooled, the solvent is removed in vacuo and the residue is chromatographed on silica gel using a gradient elution (10:90:3 to 60:40:10 EtOH–EtOAc–HOAc). Fractions containing **9** ($R_f=0.16$ (50:50:3 EtOH–EtOAc–HOAc) provide 0.39 g (51%) product. The solid is recrystallised from CH_3OH/CH_2Cl_2 (1:1) to give m.p. 225–227 °C (dec.). ^{1}H NMR ($CDCl_3$): 8.82 (*d*, $J=$ 2.3 Hz, 2H), 8.17 (*dd*, $J=$ 8.5, 2.3 Hz, 2H), 7.64 97 (*d*, $J=$ 8.5Hz, 2H), 2.93 (*s*, 12H). ^{13}C NMR (DMSO-d_6): 168.3, 152.4, 144.9, 126.4, 125.3, 121.4, 118.1, 43.4. UV (H_2O): $\lambda_{max}=421$ nm (log $\varepsilon=3.1$).

3. Results and discussion

3.1. Synthetic aspects

Of the three general approaches to the synthesis of compound **1** (Fig. 1), route A is the best. Routes A and B involve oxidative coupling of a primary amine, while route C involves a diazo coupling step. In routes B and C the *N,N*-dimethylamino group is formed before the azo linkage is generated. Routes B and C have shortcomings that counter the advantage of having the methyl groups in place at the outset. One specific shortcoming of the two routes is that both require the intermediacy of compound **3**. The synthesis **3** by the reaction of **4** with *p*-benzenediazonium sulfo-

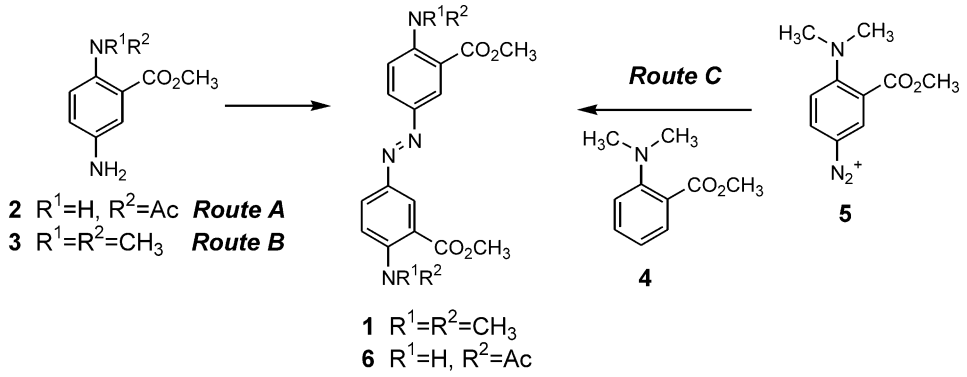

Fig. 1. Approaches to the synthesis of azo compound **1**.

nate followed by reductive cleavage of the azo group is not viable, as intermediate **4** does not couple with the diazonium salt, presumably because it is not sufficiently reactive towards electrophilic attack by a diazo compound. The coupling between **4** and **5** would suffer from the same problem. While nitration of **4** followed by reduction of the nitro group is another possible route to **3**, this reaction does not proceed cleanly under a variety of conditions. In this regard, it is known that *N,N*-dialkylaromatic compounds sometimes nitrate by an unusual electron-transfer pathway that leads to dealkyation [1].

Route A requires **2** as the precursor for introducing the azo group. The synthesis of **2** is accomplished in four steps from anthranilic acid (Fig. 2). The amino group is first protected as an acetamide, then the carboxylic acid group is esterified using dimethyl sulfate. Nitration is carried out using a mixture of nitric acid and sulfuric acid rather than the fuming nitric acid employed in a prior report [2]. The nitration product is a nearly equal mixture of the 4- and 6-nitro isomers, and recrystallisation from acetone gives the 4-nitro isomer exclusively. Finally, compound **2** is produced by catalytic hydrogenation of the nitro group.

The remaining steps employed for the conversion of **2** to **1** are shown in Fig. 3. The first step is the oxidative coupling of **2** to form the azo group. We examined this transformation in detail, especially the oxidation process utilising sodium perborate [3,4] because it normally gives the highest yield. It was anticipated that perborate coupling would be ideal, based on results from an analogous reaction involving *N*-acetyl-*p*-phenylenediamine [5], and we found that this procedure is by far the simplest and cleanest. The reaction sometimes gives the corresponding azoxy compound as a side product. In such cases the azoxy by-product is carried through the remaining steps and then separated from **1** by column chromatography.

A number of other reagents were explored for the oxidative coupling of **2**. In general, those reagents that react by oxygenation tend to give azoxy compound **7** as the major product. These include H_2O_2 in AcOH, Caro's acid (H_2SO_5), and oxone ($2KHSO_5{\cdot}KHSO_4{\cdot}K_2SO_4$). The oxidizing agents that function by hydrogen atom abstraction are more effective. Thus, the reaction of **2** with $Pb(OAc)_4$ or $PhI(OAc)_2$ gives **6** as the major product [6]. The yields are around 25%, and in the case of (diacetoxyiodo)benzene, the product mixture is contaminated with the hydrazo compound (15 mol%). Surprisingly, activated MnO_2 gives does not react with **2** [7], although activated MnO_2 is generally considered the reagent of choice for oxidative coupling of primary aryl amines.

Based on the route in Fig. 3, the next step in the synthesis of **1** is deprotection of the amino group, which is necessary for the subsequent methylation reaction. While a common method for deprotection is heating the amide in CH_3OH/aq. HCl [5], these conditions are not appropriate for **6** because they lead to hydrolysis of the ester groups. Conducting the reaction under Fisher esterification conditions (CH_3OH/H_2SO_4) is the method of choice, as the methyl esters groups are preserved.

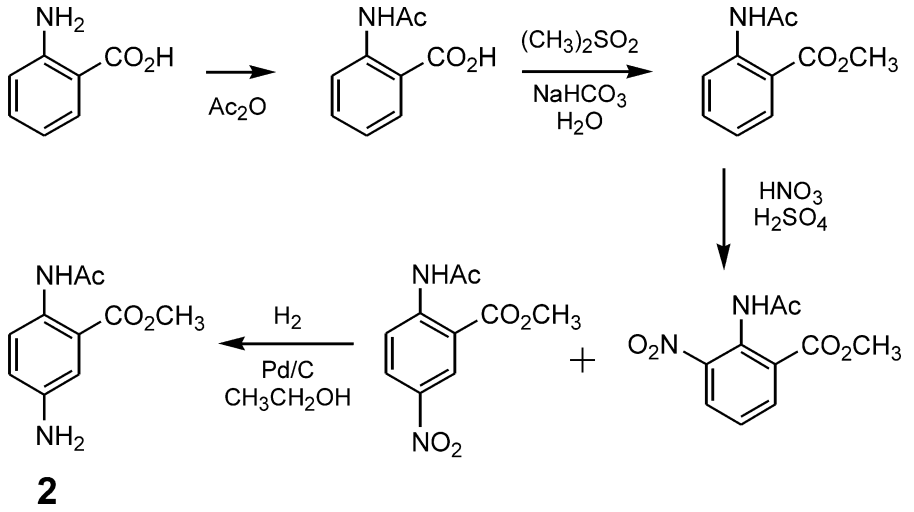

Fig. 2. Synthesis of compound **2** from anthranilic acid.

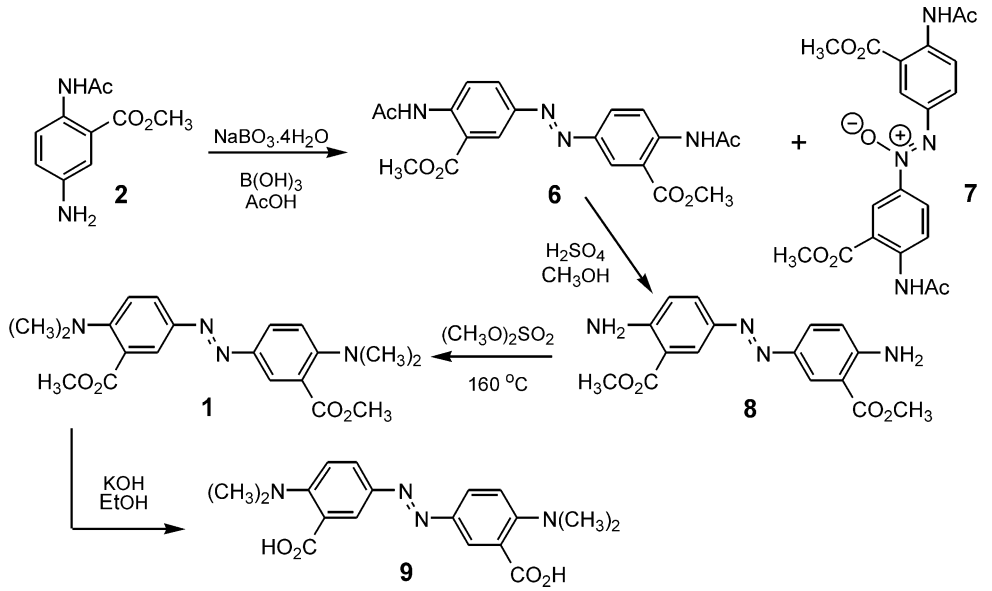

Fig. 3. Synthesis of azo compounds **8**, **1** and **9** from **2**.

Direct methylation of **8** using CH_3I and K_2CO_3 does not work, but it works in part when aqueous $(CH_3O)_2SO_2$ and $NaHCO_3$ [8] is used. Reductive amination using a mixture of CH_2O and H_2SO_4/$NaBH_4$ [9] or $ZnCl_2/Zn(BH_4)_2$ [10] gives mainly mono-methylation, even when an excess of the methylating agent is employed. The ultimately successful method involves heating **8** in excess $(CH_3O)_2SO_2$ at 160 °C for several minutes. This approach gives mainly *N*-dimethylation with some *N*-trimethylated by-products. No doubt one reason for the sluggishness of this reaction is the electron-withdrawing effects of the *ortho*-carbomethoxy group. The fact that the standard methods introduce only one methyl group suggests that steric factors inhibit dimethylation.

3.2. Dye properties

The absorption maxima for the neutral and protonated forms of azo compounds **1**, **8** and **9** as well as the pK_a values for the latter forms are shown in Table 1. The hypsochromic shift of the absorption maxima of **1** and **9** vs. **8** is consistent with the stronger electron-donating ability of the NMe_2 group vs. the NH_2 group [11]. The contrasting absorption properties of the protonated forms (halochroism) demonstrates that there are two basic sites in these azo compounds [12]. Both **8** and **9** protonate preferentially at the azo nitrogen to give azonium ions, whereas **1** protonates mainly at the amino group to give ammonium ions (Fig. 4).

The reported pK_a values are somewhat lower than those for the protonated mono-aminoazobenzenes, which fall in the range of 1.8–2.5 [13]. Lower values are expected because of the electron-withdrawing effect of the two carboxylate groups. The difference in the absorption maxima for the neutral and azonium forms of a number of dimethylaminoazobenzenes follows the Hammett equation [11]. In this case, we extrapolated the Hammett relationships to compound **9** by assuming that the substitutents effects are additive. The observed difference in the absorption maxima for **9** and **9**-H^+ is only 71 nm, whereas the calculated difference is 151 nm [14]. Comparing the absorption maxima of **9**-H^+ with those of some previously reported dimethylaminoazobenzenes reveals that the observed absorption maximum of **9**-H^+ is rather hypsochromic. Most azonium ions absorb above 500 nm.

Two other aspects of the protonation experiments are noteworthy. Compound **8** forms a doubly protonated species that has an absorption maximum of 496 nm and pK_a of ca. −0.5. The absorption spectrum of **9** in solution without acid does not intersect the isosbestic point of solutions of **9** containing acid. We found that the absorption maximum of **9** is not shifted after the addition of acid but it is more intense. Presumably, the carboxylic acid groups are partially ionized in neutral solution.

Table 1
pH Properties of azo dyes **1**, **8** and **9**

Dye	λ_{max} B: (nm)	λ_{max} B:H^+ (nm)	pK_a
1	435	310	1.20[a]
8	388	577	0.10[a]
9	421	492	0.72[b]

[a] Acidity determination performed in 50% aq. EtOH.
[b] Acidity determination performed in H_2O.

3.3. Theoretical calculations

The use of theoretical calculations in the prediction of dye properties is becoming more prevalent. For example, the PPP and ZINDO methods are useful for predicting absorption properties [15,16] and semi-empirical calculations are appropriate for geometry optimisations [16–18]. Relevant to this paper is the application of semi-empirical calculations for predicting the relative energies of azonium and ammonium ion tautomers of protonated aminoazobenzenes [19].

Both AM1 and PM3 methods are reasonably robust in their ability to predict the properties

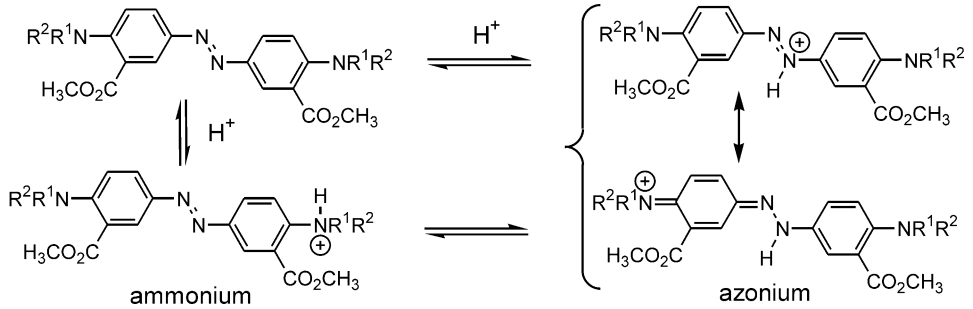

Fig. 4. Ammonium/azonium ion tautomerization involving type **1** azo compounds.

of azo disperse dyes, with each method having limitations. For example, the AM1 method predicts the *cis*-azo geometry to be more stable than the *trans*-azo geometry [16]. This problem is probably related in part to the underestimation of π-interaction energies [17]. AM1 also does not treat H-bonding properly. The most serious problem with PM3 is its tendency to pyramidalize arylamino groups [16]. All of these tendencies impacted our results.

The heats of formation for **1**, **8** and **9** and the corresponding ammonium and azonium conjugate acids were calculated with the AM1 and PM3 semi-empirical methods using PC Spartan Pro® software. We report two ΔH_f values for each calculation. The upper entry is the gas-phase value, while the lower entry is the solution phase value, which is the sum of the gas-phase and SM5.4 solvation energy values. The solvation model 5 (SM5) is a model for aqueous solvation of organic compounds that accounts for both electrostatic effects and first solvation shell effects [20]. The energies of a number of conformations for each molecule were calculated, but only the lower energy structures are reported. Each calculated structure can be characterized by a set of dihedral angles ϕ_1–ϕ_4 defined in Fig. 5. All calculated structures were initially input as the *trans* azo structure since the *cis* geometry is less stable. In most of the structures, the two aryl groups and the azo group are coplanar and thus fully conjugated. The presence of the carboxylate group *meta* to the azo groups gives rise to rotational isomerism about the N–C4 bond. For conjugated structures the carboxylate and the azo groups can point in opposite directions ($\phi_4 = 180°$) or in the same direction ($\phi_4 = 0°$). This isomerism gives rise to four rotomers about the C1–N and C1′–N bonds (ϕ_4–$\phi_{4'}$): 180–180°, 0–180°, 0–0°, and 180–0°. For **1**, **8** and **9** the 180–180° and 0–0° rotomers have C2 symmetry, and the 180–0° and 0–180° rotomers are identical. The symmetry of the 180–180° and 0–0° rotomers and the equivalency of the 180–0° and 0–180° rotomers are broken in the protonated forms. The aryl groups are quite different in the protonated forms. In these cases two rows of dihedral angles are reported in the tables. The upper row refers to the half bearing the proton.

3.3.1. Dye *8*

The ΔH_f values for several conformations of **8** and **8**-H^+ are reported in Table 2. In all cases, the O–CH_3 bond is *anti* to the C3–C(=O) bond ($\phi_1 = 180°$). In most structures the carbonyl group and the aryl ring are nearly coplanar with the carbonyl oxygen closest to one of the amino hydrogen atoms, with $|\phi_2| \leqslant 10°$. AM1 calculations predict that the amino group in **8** is flat and coplanar with the aryl ring ($|\phi_3| \leqslant 2$, $\phi_5 = 1$), while PM3 calculations show significant pyramidalization

Z,Z' = lone pair (**1**, **8**, **9**), or
Z = lone pair, Z' = H (azonium form), or
Z = H, Z' = lone pair (ammonium form)
R = H (**8**) or CH_3 (**1** and **9**)
R^1 = H (**9**) or CH_3 (**1** and **8**)

ϕ_1 = C3-C(O)-O-R^1
ϕ_2 = C4-C3-C=O
ϕ_3 = min C3-C4-N-R(H)
ϕ_4 = C2-C1-N=N
ϕ_5 = sp^3-N pyramidal angle

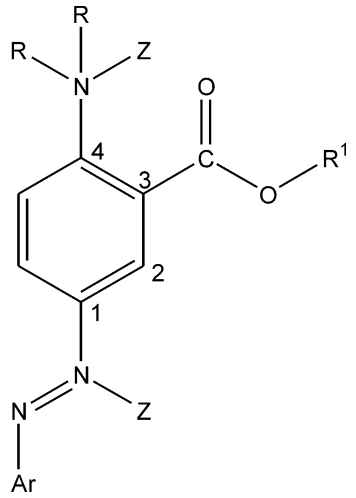

Fig. 5. Definition of angles employed in modeling studies.

Table 2
Semi-empirical heats of formation for azo compounds **8** and **8**-H^{+} [a,b,c,d,e]

	ΔH_f						ΔH_f					
8	AM1	ϕ_1	ϕ_2	ϕ_3	ϕ_4	ϕ_5	PM3	ϕ_1	ϕ_2	ϕ_3	ϕ_4	ϕ_5
a	−76.6	180	1	−2	−178	1	−75.3	180	10	−20	180	15
	−87.7						−86.1					
b	−76.5	180	1	−2	0	1	−75.3	180	10	−20	1	15
	−88.6				180		−86.2				−178	
c	−76.6	180	−1	1	0	1	−75.3	180	10	−20	0	15
	−88.5						−86.3					
***8*-*H*$^{+}$**												
a	72.6	180	0	0	180	0	77.9	180	−2	12	179	8
	24.2	180	0	0	−179	0	29.2	180	0	0	180	0
b	72.7	180	1	0	1	0	77.9	180	−1	12	0	7
	24.2	180	0	0	180	0	29.6	180	0	1	180	0
c	72.5	180	0	0	0	0	78.1	180	−1	11	0	7
	24.2	180	1	0	0	0	30.5	180	0	1	0	0
d	72.4	180	0	0	180	0	78.2	180	−1	12	180	7
	23.8	180	0	0	0	0	30.1	180	0	0	0	0
a′	77.5	180	−3	44	150	19	73.0	180	0	0	121	20
	14.2	180	1	0	177	0	11.0	180	5	−18	178	12
b′	77.5	180	−2	43	−36	19	73.0	180	1	0	−82	20
	14.1	180	1	0	177	0	11.0	180	4	−18	180	12
c′	77.5	180	−3	43	−37	19	73.1	180	−1	0	83	20
	13.5	180	0	0	4	0	10.9	180	5	−18	−1	12
d′	77.5	180	−3	44	148	19	73.0	180	0	0	115	20
	12.9	180	0	0	−4	0	10.9	180	5	−18	−3	12

[a] The energy units are kcal/mol.
[b] The bottom of the two ΔH_f entries includes the SM5.4 solvation energy.
[c] The first set of **8**-H^{+} entries are azonium structures, while the second set (primed entries) are ammonium structures.
[d] For each **8**-H^{+} entry the top row of dihedral angles is for the protonated aryl portion
[e] ϕ_3 for the protonated aryl portion of the ammonium structures is the C3–C4–N–H dihedral.

($\phi_5 = 15$) even when a planar structure is employed in the calculations. In the PM3 structures the carbonyl group is twisted slightly out of plane, to retain close proximity with the amino hydrogen atom, and the amino group lone pair is fully conjugated with the aryl π-system.

The aryl groups and the azo linkage are fully conjugated ($\phi_4 = 0$ or 180°). There is little difference in the energies of the various structures produced by rotating about the C1–N(=N) bond. The dihedral angles of the AM1 calculated azonium ion structures are not significantly different from those of compound **8** itself, whereas the PM3 calculated structures change significantly. In the latter, the amino N-atom on the non-protonated half becomes fully planar. The change in hybridization

of the amino N-atom is reasonable due to the importance of the azonium ion resonance structure in which this atom is part of an unsaturated group (Fig. 4). Interestingly, the other amino N-atom also becomes partially planar. The largest energy difference among the protonated rotomers of **8** is only 1.3 kcal/mol. The structural changes caused by protonation of **8** are more pronounced with the ammonium ions than with the azonium ions. Because the ammonium group is tetravalent, it is necessarily pyramidalized ($\phi_5 = 19$–20°).

None of the AM1 calculated structures show H-bonding between the adjacent carbonyl and ammonium groups. Although the carbonyl group remains in plane, the ammonium group is twisted out of plane, thus preventing interaction with the carbonyl group ($\phi_3 = 43$–44°). Also, the aryl ammonium moiety is twisted about the C1–N bond by up to 37°, thus reducing its conjugation with the rest of the molecule. In contrast, the calculated PM3 structures indicate H-bonding between the carbonyl and ammonium groups ($\phi_2 = \phi_3 = 0$). The aryl ammonium moiety is more twisted (by up to 83°) in the PM3 structures than the AM1 structures. The difference in energy between the azonium and ammonium forms was determined using the minimum energy for each set of structures. The azonium ion has a lower gas-phase AM1 energy (−5.1 kcal/mol, Table 6), but the ammonium ion is lower in energy when solvent-corrected AM1 calculations and the PM3 calculations conducted. Calculations using the solvation model show a great preference for the ammonium ion over the azonium ion.

3.3.2. *Dye* ***1***

The structures for **1** and **1**-H^+ show greater structural variation than those of **8** and **8**-H^+ because the extra methyl groups force the dimethylamino group to twist out of the molecular plane. Table 3 reports the structural parameters and ΔH_f values for several conformations of **1** and **1**-H^+. As observed in **8**, the O–Me bond in **1** is *anti* with respect to the C3–C(=O) bond ($\phi_1 = 180^\circ$). The results of AM1 calculations indicate that the carbonyl group prefers to point toward the dimethylamino group ($\phi_2 = 40^\circ$ in **1a**–**c** vs. $\phi_2 = -112^\circ$ in **1d** which is less stable). This preference is much less evident in the PM3 calculated structures, as the carbonyl group is nearly perpendicular to the aryl ring. The dimethylamino and carbonyl groups are twisted by similar amounts using each method ($\phi_3 \sim 36^\circ$ and -111 for AM1 and PM3, respectively), with the lone pair on the amino group pointing toward the carbonyl group. The N-atom of the dimethylamino group shows more pyramidalization in the AM1 structures of **1** than in **8** (5° vs. 1°). The PM3 structures have highly pyramidalized N-atoms in both **1** and **8**. The energies of the rotomers involving the C1–N(=N) bond of **1** are within 1.0 kcal/mol of each other. The azonium ion structures of **1**–H^+ all show a planar dimethylamino group. The AM1 structures are fully planar ($\phi_5 \sim 0^\circ$), whereas the PM3 structures are fully planar for the amino group that can delocalise its lone pair to the cationic azonium N-atom, and only partially planar for the other ($\phi_5 = 7^\circ$). In the case of protonated **1**, both dimethylamino groups are twisted toward the molecular plane from their orientation in **1**, but the conjugated amino group is more twisted. The carbonyl groups are out of plane in the protonated and neutral forms. The greatest energy difference between rotomeric azonium ions is observed with the PM3/SM5.4 energies of **1**-H^+**b** and **d** (1.8 kcal/mol). The low energy ammonium structures (**1**-H^+**a′**–**d′**) show H-bonding between the ammonium group and the adjacent carbonyl ($\phi_2 = \phi_3 = 0^\circ$), even in the AM1 calculated structures. The ammonium aryl group is twisted out of the plane of the remaining azoaryl moiety (ϕ_4, upper entry, deviates from 0 or 180°). The dimethylamino group of the other aryl ring is slightly twisted from the molecular plane, and the amino group becomes planar in the AM1 structures. Structure **1**-H^+**e′** shows that H-bonding to the methoxy O-atom is less favorable compared to the H-bonding involving the carbonyl O-atom. Structure **1**-H^+**f′** shows that breaking the H-bond (ϕ_3, upper entry, initially set to 180°) produces a less stable structure. The energies of ammonium group rotomers **1**-H^+**a′**–**d′** differ by no more than 1.2 kcal/mol. Results of these calculations indicate that the ammonium form is more stable (Table 6).

3.3.3. Dye **9**

Dye **9** shows the greatest structural variability with regards to modeling. The O–H group can be *anti* to the C3–C(=O) bond, or it can be *syn* and participate in H-bonding with the amino N-atom when $\phi_2 \sim 180°$. Data for both sets of structures for **9** are shown in Table 4. For the calculations performed, conformers **9a**–**c** were input as *anti* structures with coplanar carbonyl groups ($\phi_2 = 0°$), but the optimized structures have carbonyls that are partially (AM1) or completely twisted (PM3). Conformers **9d** and **e** were input with the O–H bond *syn* to the C3–C(=O) bond and pointed towards the amino N-atom ($\phi_2 = 180°$). The H-bond

Table 3
Semi-empirical heats of formation for azo compounds **1** and **1**-H$^+$ [a,b,c,d,e]

	ΔH_f						ΔH_f					
1	AM1	ϕ_1	ϕ_2	ϕ_3	ϕ_4	ϕ_5	PM3	ϕ_1	ϕ_2	ϕ_3	ϕ_4	ϕ_5
a	−42.1	−176	41	36	177	5	−73.3	179	90	−111	179	16
	−49.2						−78.7					
b	−42.1	−176	41	36	−4	5	−73.2	179	89	−110	−1	16
	−50.1				176		−78.8				179	
c	−42.2	−176	41	35	−6	5	−73.3	179	90	−111	1	16
	−49.9						−78.9					
d	−40.8	178	−112	36	0	7	−73.1	−179	−84	96	−8	16
	−50.2				179		−78.4				171	
***1*-H$^+$**												
a	105.5	−178	42	19	177	1	87.1	−179	73	29	179	7
	66.1	−176	40	12	180	0	44.2	−177	68	10	179	0
b	105.5	−177	44	19	−2	1	87.0	−178	73	29	−2	7
	66.0	−176	40	13	180	0	43.4	−177	69	10	179	0
c	105.4	−177	44	18	−2	1	87.2	−179	74	28	−2	7
	66.1	−177	39	13	−3	1	44.6	−179	68	11	−2	0
d	105.3	−178	43	19	179	1	87.1	−179	73	29	180	7
	65.7	−177	39	13	−3	1	45.2	−179	70	11	−2	1
a	102.9	180	0	0	150	18	78.3	180	−1	0	110	18
	58.9	−177	44	21	176	1	34.4	178	91	−84	179	15
b′	102.9	180	0	0	40	18	78.6	180	0	0	85	18
	58.8	−177	45	21	−177	1	34.3	178	99	107	176	16
c′	102.8	180	0	0	−37	18	78.3	180	0	0	−86	18
	58.2	−177	44	21	−5	1	34.3	180	92	−84	2	15
d′	102.8	180	0	0	149	18	78.4	180	0	0	172	18
	57.7	−177	45	21	−5	1	34.1	178	97	−113	0	16
e′	106.9	175	−151	11	149	18	83.3	179	−152	−4	82	18
	59.2	−177	44	21	176	1	34.7	178	89	−86	180	15
f′	108.7	176	−29	−170	146	16	84.6	176	−46	−178	180	17
	61.6	−177	45	20	175	1	34.7	178	91	144	178	15

[a] The energy units are kcal/mol.
[b] The bottom of the two ΔH_f entries includes the SM5.4 solvation energy.
[c] The first set of **1**-H$^+$ entries are azonium structures, while the second set (primed entries) are ammonium structures.
[d] For each **1**-H$^+$ entry the top row of dihedral angles is for the protonated aryl portion
[e] ϕ_3 for the protonated aryl portion of the ammonium structures is the C3–C4–N–H dihedral.

is retained in the PM3 optimized structures, but not in the AM1 optimized structures. Even though the AM1 optimized structures indicate poor H-bonding, the amino groups become more pyramidal. While **9d** and **e** are significantly higher in energy than **9a–c** following AM1 and AM1/SM5.4 calculations, they have nearly the same stability following PM3 calculations and the PM3/SM5.4 calculated structures are more stable by nearly 70 kcal/mol.

Because the aryl groups are different in **9**-H^+, there are many structures to consider (Table 5). Five azonium structures for each rotomer about the C1–N(=N) bond are reported. The initial structures for **9**-H^+**a,c,e,g** are input with *anti* O–H bonds and carbonyl groups that pointed towards the amino groups. The carbonyl groups are all twisted out of the molecular plane in the optimized structures. The N-atom of the dimethylamino groups is completely planar following AM1 calculations but the PM3 calculated structures have partially planar N-atoms. The dimethylamino groups in **9**-H^+**a,c,e,g** are twisted towards the molecular plane relative to **9**, especially those conjugated with the cationic azonium N-atom. Azonium ion structures **9**-H^+**b,d,f,h** have one (AM1 and first PM3 calculation) or two (second PM3 calculation) H-bonds between the O–H (syn to C3–C(=O)) and the dimethylamino groups. In the structures with a single H-bond, the bond involves the unconjugated amino group. The H-bond is poorly formed in the AM1 calculated structures, but well defined in the PM3 derived structures. No AM1 calculated structures with two H-bonds are reported because the effect of having just one H-bond is to raise the AM1 calculated heat of formation. The increase in the energy from PM3 calculations is small when shifting from zero to one H-bond, but much larger when shifting from one to two H-bonds, where the conjugated N-atom is H-bonded. However, H-bonding in the solvation-corrected PM3 calculated structures leads to energy decreases on the order of 30 kcal/mol per H-bond. Rotational isomers **9**-H^+**d** and **9**-H^+**f** differ by 2.5 kcal/mol, but there is little difference among the rest. Fewer ammonium structures are reported because H-bonding between the ammonium group and the carbonyl group is favored. H-bonding is present even in the AM1 calculated structures. The ammonium aryl group is twisted out of conjugation with the rest of the molecule, especially in the PM3 calculated structures. For those structures in which the dimethylamino group on the other aryl ring does not participate in H-bonding, the carbonyl groups

Table 4
Semi-empirical heats of formation for azo compounds **9**[a,b]

9	ΔH_f AM1	ϕ_1	ϕ_2	ϕ_3	ϕ_4	ϕ_5	ΔH_f PM3	ϕ_1	ϕ_2	ϕ_3	ϕ_4	ϕ_5
a	−55.7 −67.5	−176	36	36	177	5	−88.7 −99.0	179	90	−114	155	16
b	−55.7 −68.3	−176	37	36	−2 179	5	−88.8 −99.3	179	91	−113	−8 176	16
c	−55.7 −68.2	−176	37	36	−2	5	−88.8 −99.5	178	91	−112	−11	16
d	−50.9 −63.8	4	126	−66	−176	13	−90.0 −167.3	0	180	116	180	16
e	−50.5 −65.2	3	125	−66	−13 171	13	−89.1 −167.4	0	179	116	0 −178	16
f	−50.8 −64.6	4	126	−66	0	13	−89.9 −167.8	0	180	116	0	16

[a] The energy units are kcal/mol.
[b] The bottom of the two ΔH_f entries includes the SM5.4 solvation energy.

Table 5
Semi-empirical heats of formation for azo compounds **9**-H^{+}[a,b,c,d,e]

	ΔH_f						ΔH_f						ΔH_f					
9-H^{+}	AM1	ϕ_1	ϕ_2	ϕ_3	ϕ_4	ϕ_5	PM3	ϕ_1	ϕ_2	ϕ_3	ϕ_4	ϕ_5	PM3	ϕ_1	ϕ_2	ϕ_3	ϕ_4	ϕ_5
a	93.5	−178	38	20	−176	1	72.7	−178	70	29	179	7						
	47.7	−176	36	13	−176	0	24.2	−176	65	11	179	0						
b	98.7	0	126	−34	−174	6	73.4	0	180	−115	−178	16	81.0	0	180	115	180	16
	50.4	−176	36	12	180	0	−8.7	−176	62	10	180	0	−40.2	−1	−179	115	180	16
c	93.5	−177	40	−164	0	1	72.7	−177	72	28	−1	7						
	47.7	−176	36	−168	180	0	23.6	−176	65	11	179	0						
d	98.8	0	124	−33	0	6	74.1	0	180	−115	0	16	82.1	0	180	115	−1	16
	50.8	−176	36	12	180	0	−9.1	−176	62	10	179	0	−40.4	0	180	115	179	16
e	93.3	−177	39	19	−3	1	72.8	−178	72	28	0	7						
	47.8	−177	34	14	−4	1	24.6	−178	64	13	−2	1						
f	98.6	0	124	−33	2	6	74.2	0	180	115	0	16	79.6	0	180	115	−1	16
	51.0	−176	36	12	−3	1	−8.1	−178	61	10	−3	0	−40.8	0	180	116	0	16
g	93.3	−178	38	20	178	1	72.8	−178	70	29	180	7						
	47.5	−177	34	14	−4	1	25.1	−178	64	13	−2	1						
h	98.6	0	125	−34	−179	6	73.9	0	180	116	179	16	79.9	0	180	115	179	16
	50.0	−177	34	13	−4	0	−8.0	−177	61	10	−3	0	−40.1	0	180	115	0	16
a′	91.0	179	0	0	150	18	64.1	180	0	0	99	18	64.1	180	0	0	117	18
	43.9	−177	39	22	176	1	12.8	178	91	−84	179	16	−20.5	0	180	116	180	16
b′	91.1	180	0	0	−36	18	63.8	180	0	0	−95	18	64.1	180	0	0	−89	18
	43.8	−177	40	21	176	1	12.8	178	91	−84	−179	15	−20.5	0	180	115	−179	16
c′	91.1	180	0	0	4	18	63.7	180	−1	0	91	18	63.8	180	0	−1	87	18
	43.2	180	40	21	−1	1	12.7	178	92	−84	−1	15	−20.9	1	179	116	−1	16
d′	91.0	180	1	0	−149	18	63.7	180	0	0	104	18	63.7	180	−1	0	104	18
	42.9	−177	40	21	3	1	12.6	178	92	−84	−1	15	−20.9	0	180	116	1	16

[a] The energy units are kcal/mol.
[b] The bottom of the two ΔH_f entries includes the SM5.4 solvation energy.
[c] The first set of **9**-H^{+} entries are azonium structures, while the second set (primed entries) are ammonium structures.
[d] For each **9**-H^{+} entry the top row of dihedral angles is for the protonated aryl portion
[e] ϕ_3 for the protonated aryl portion of the ammonium structures is the C3–C4–N–H dihedral.

are as twisted as they are in **9**, while the dimethylamino groups are slightly less twisted. The ammonium ions possessing one and two H-bonded dimethylamino groups have nearly identical PM3 energies, but their PM3/SM5 energies favor the structures with two H-bonds by over 30 kcal/mol. Results of AM1 calculations indicate that the azonium ion is only slightly higher in energy than the ammonium ion in the gas phase (Table 6). Results of PM3 calculations predict the energy gap to be much larger in the gas phase. However, the solution phase energies greatly favor the azonium ion, especially when H-bonds between both carboxylic acid and amino groups are present.

Table 6
Semi-empirical heats of reaction for the ammonium/azonium ion tautomerisation[a]

	8		1		9		
	AM1	PM3	AM1	PM3	AM1	PM3	PM3
Gas phase	−5.1	4.9	2.5	8.8	2.3	8.9	15.8
SM5.4	10.9	18.3	7.9	9.3	4.6	−21.8	−19.9

[a] The energy units are kcal/mol.

3.3.4. Discussion

The results of these theoretical calculations provide an explanation for why azo compound **1** forms an ammonium ion, whereas **8** and **9** form azonium ions. The azonium structure is favored in the case of **8** because the amino groups are fully conjugated with the extended π-electron system. Electron donation from the amino groups to the azonium moiety stabilizes the azonium structure. Out-of-plane twisting of the dimethylamino groups in **1** diminishes resonance stabilization of the azonium form, favoring the ammonium structure. Similar behavior has been noted in some nitrophenyldiamines where out-of-plane twisting of a dimethylamino group due to an adjacent nitro group results in unusually low molar absorptivities [15]. In the case of **9**, the carboxylic acid groups can H-bond with the dimethylamino groups. Although the SM5 calculations give a very high solvation energy for this interaction, it is reasonable that the solvation energy would determine which structure is favored in solution. The azonium ion retains both H-bonds between the carboxylic acids and the dimethylamino groups, while the ammonium ion must lose one to form a H-bond between the ammonium group and the carbonyl oxygen. The protonated N-atom of the azonium ion is not a solvation site for the ammonium ion, making the azonium ion more stable. One consequence of this argument is that the amino groups of the azonium ion are poorly conjugated with the extended π-electron system. The above mentioned unusual bathochromic shift of the azonium form of **9**-H^+ supports the involvement of a less-extended π-electron system.

4. Conclusions

The conjugation and proximity of the amino and the carboxyl groups in 3,3′-bis(carbomethoxy)-4,4′- bis-(dimethylamino)azobenzene, 3,3′-bis(carbomethoxy)-4,4′-diaminoazobenzene and 4,4′-bis(dimethylamino)azobenzene-3,3′-dicarboxylic acid produce unusual dye properties as well as to synthetic challenges. In this regard, 3,3′-bis(carbomethoxy)-4,4′-bis-(dimethylamino)azobenzene stands out because its conjugate acid is an ammonium ion and its synthesis by methylation of 3,3′-bis(carbomethoxy)-4,4′-bis-(dimethylamino)azobenzene requires forcing conditions. In contrast, the fact that 4,4′-bis(dimethylamino)azobenzene-3,3′-dicarboxylic acid gives an azonium ion as its conjugate acid is ascribed to H-bonding between the carboxylic acid and dimethylamino groups.

Acknowledgements

This work was supported by a grant from the National Institutes of Health.

References

[1] Loeppky RN, Singh SP, Elomari S, Hastings R, Theiss TE. J Am Chem Soc 1998;120:5193.
[2] Adams R, Young TE, Short RWP. J Am Chem Soc 1954; 76:1114.
[3] Ogata Y, Shimizu H. Bull Chem Soc Jpn 1979;52:635.
[4] Huestis L. J Chem Ed 1977;54:327.
[5] Santurri P, Robbins F, Stubbings R. Org Synth 1973; V:341.
[6] Pausacker KH, Scroggie JG. J Chem Soc 1954:4003.
[7] Barakat MZ, Abdel-Wahab MF, El-Sadr MM. J Chem Soc 1956:4685.
[8] Hηnig S, Quast H, Brenninger W, Frankenfeld E. Org Synth 1973;V:1018.
[9] Giumanini AG, Chiavari G, Musiani MM, Rossi P. Synthesis 1980:743.
[10] Bhattacharyya S, Chatterjee A, Duttachowdhury SK. J Chem Soc Perkin Trans 1994;1:1.
[11] Yagupol'skii LM, Gandel'sman LZ. J Gen Chem USSR 1965;35:1259.
[12] Zollinger H. Azo and diazo chemistry: aliphatic and aromatic compounds. New York: Interscience, 1961. p. 328–37.
[13] Bershtein IYa, Ginzburg OF. Russ Chem Rev 1972; 41:97.

[14] This value was obtained using the equation $\Delta = 120 - 101\sigma_p - 76\sigma_m$ with one dimethylamino group ($\sigma_p = -0.83$) and two carboxylate groups ($\sigma_m = 0.35$).
[15] Griffiths J. Dyes and Pigments 1982;3:211.
[16] Lye J, Freeman HS, Hinks D. In: Cisneros G, Cogordan JA, Castro M, Wang C., editors. Computational chemistry and chemical engineering. Singapore: World Scientific, 1997. p. 214–26.
[17] Lye J, Freeman HS, Hinks D. Textile Res J 1999;69:583.
[18] Lye J, Freeman HS, Cox RD. Dyes and Pigments 2000; 47:53.
[19] Liwo A, Tempczyk A, Widernik T, Klentak T, Czermiński J. J Chem Soc Perkin Trans 1994;2:71.
[20] Chambers CC, Hawkins GD, Cramer CJ, Truhlar DG. J Phys Chem 1996;100:16385.